HHS Public Access

Author manuscript

Mol Psychiatry. Author manuscript; available in PMC 2019 March 25.

Published in final edited form as:

Mol Psychiatry. 2018 February ; 23(2): 282–294. doi:10.1038/mp.2017.164.

Prenatal one-carbon metabolism dysregulation programs schizophrenia-like deficits

A Alachkar[1,7], **L Wang**[1,7], **R Yoshimura**[1], **AR Hamzeh**[2], **Z Wang**[1], **N Sanathara**[1], **SM Lee**[1], **X Xu**[3], **GW Abbott**[1,4], and **O Civelli**[1,5,6]

[1]Department of Pharmacology, School of Medicine, University of California, Irvine, Irvine, CA, USA

[2]Centre for Arab Genomic Studies, Dubai, United Arab Emirates

[3]Department of Anatomy & Neurobiology, School of Medicine, University of California, Irvine, Irvine, CA, USA

[4]Department of Physiology and Biophysics, School of Medicine, University of California, Irvine, Irvine, CA, USA

[5]Department of Pharmaceutical Sciences, School of Medicine, University of California, Irvine, Irvine, CA, USA

[6]Department of Developmental and Cell Biology, School of Medicine, University of California, Irvine, Irvine, CA, USA.

[7]These authors contributed equally to this work.

Abstract

The methionine-folate cycle-dependent one-carbon metabolism is implicated in the pathophysiology of schizophrenia. Since schizophrenia is a developmental disorder, we examined the effects that perturbation of the one-carbon metabolism during gestation has on mice progeny. Pregnant mice were administered methionine equivalent to double their daily intake during the last week of gestation. Their progeny (MET mice) exhibited schizophrenia-like social deficits, cognitive impairments and elevated stereotypy, decreased neurogenesis and synaptic plasticity, and abnormally reduced local excitatory synaptic connections in CA1 neurons. Neural transcript expression of only one gene, encoding the Npas4 transcription factor, was >twofold altered (downregulated) in MET mice; strikingly, similar *Npas4* downregulation occurred in the prefrontal cortex of human patients with schizophrenia. Finally, therapeutic actions of typical (haloperidol) and atypical (clozapine) antipsychotics in MET mice mimicked effects in human schizophrenia

Correspondence: Dr A Alachkar, Department of Pharmacology, School of Medicine, University of California, Irvine, 355 Med Surge II Irvine, CA 92697-4625, USA. aalachka@uci.edu.

AUTHOR CONTRIBUTIONS

AA and OC conceived the project and wrote the manuscript. AA, OC and LW designed the experiments. AA, LW, RY, SML and ZW conducted the experiments, ARH carried out the genetic analyses, XX and GWA supervised the transcriptomic and electrophysiological studies and helped with the preparation of the manuscript.

CONFLICT OF INTEREST

The authors declare no conflict of interest.

Supplementary Information accompanies the paper on the Molecular Psychiatry website (http://www.nature.com/mp)

patients. Our data support the validity of MET mice as a model for schizophrenia, and uncover methionine metabolism as a potential preventive and/or therapeutic target.

INTRODUCTION

The one-carbon metabolism plays a critical role in the integration of genetic and environmental factors. This universal pathway cycles methyl groups from methionine to various products. Methionine, supplied through the diet, is converted to S-adenosylmethionine (SAM) the main methyl donor, and is used by over 100 methyltransferases. Substrates can be DNA, RNA, proteins, phospholipids, carbohydrates and neurotransmitters, making the one-carbon metabolism a key player in almost all cellular functions (Figure 1a)[1–5] that serves specific needs of different tissues and different developmental stages.[6]

The potential contribution of the one-carbon metabolism to the pathophysiology of schizophrenia is supported by data dating back to the sixties. High methionine administration exacerbates the psychotic symptoms in patients with schizophrenia.[7,8] Dysfunction in the one-carbon metabolism has also been shown to lead to (1) an abnormal metabolism of dopamine, noradrenaline and serotonin,[9] (2) abnormal DNA methylation and (3) increased toxic plasma homocysteine. Deficiencies in the one-carbon metabolism components folate and vitamin B_{12}, and hyperhomocysteinemia, are consistent findings in schizophrenia patients.[10,11] The link between the one-carbon pathway and schizophrenia is also reflected in the strong association between the genes encoding transmethylation enzymes such as methylenetetrahydrofolate reductase, catechol-O-methyltransferase, methionine adenosyltransferase, methionine synthase and DNA methyltransferase, and schizophrenia.[12–18]

Diets that change the one-carbon metabolism during pregnancy influence the methylation reactions and lead to permanent changes in offspring phenotypes.[19–21] Folate deficiency during pregnancy has long been known as a risk factor for schizophrenia.[22] Recently, a study of seasonal fluctuations in the dietary intake of rural Gambian women showed that maternal methyl-donor nutrient intake during conception influences plasma methyl-donor pathway substrates that predict changes in methylation at metastable epialleles in the offspring DNA.[20,23] Most significantly, the occurrence of maternal hyperhomocysteinemia during the third trimester of pregnancy is associated with a twofold increase in the risk of schizophrenia in offspring.[24]

In spite of the strong evidence for a central role of the one-carbon metabolism in the pathophysiology of schizophrenia, a study of its role in schizophrenia during gestation has not previously been undertaken. Here we examine the causal role that dysregulation of the one-carbon metabolism during prenatal stages has on the pathophysiology of schizophrenia. We test the hypothesis that the increase in prenatal methionine load leads to permanent deficits in behavioral responses that are associated with schizophrenia. We also investigate the translational aspect of this animal model in the pathogenesis of schizophrenia in humans.

MATERIALS AND METHODS

Animals and breeding procedures

Swiss Webster mice, 8–9 weeks age, were obtained from Charles River Laboratories (Wilmington, MA, USA). One male and two female mice were group-housed for harem breeding and maintained on a 12-h light/dark cycle (light on at 0700 hours) with food and water available ad libitum. Pregnant mice were individually housed from the 13 day of pregnancy (gestational day 13) until delivery. After weaning (postnatal day 21), male mice were selected for the study and group-housed separately. All experimental procedures were approved by the Institutional Animal Care and Use Committee of University of California, Irvine and were performed in compliance with national and institutional guidelines for the care and use of laboratory animals.

Drug administration

L-methionine (MET, Sigma-Aldrich, St. Louis, MO, USA) was dissolved in saline. Haloperidol (HAL, Research Biochemicals International) and clozapine (CLZ, Sigma-Aldrich) were dissolved in saline with 0.3% tartaric acid, after which the pH was adjusted to pH 5–6 with sodium hydroxide. Pregnant mice that mated with the same male mouse were administered with MET (750 mg/kg, 15 ml/kg, s.c.) or saline (SAL) twice a day (0900/1500 hours) for 7 to 8 consecutive days from the 14 day of pregnancy (gestational day 14) until delivery. The daily dose of methionine injected was twofold that of the normal daily dietary methionine intake. In the locomotion and social interaction tests, haloperidol (0.1 mg/kg, 5 ml/kg, i.p.) and clozapine (1.0 mg/kg, 5 ml/kg, i.p.) were administered 40 and 60 min before the test, respectively. In the prepulse inhibition test, haloperidol (0.25 mg/kg, 5 ml/kg, i.p.) and clozapine (2.5 mg/kg, 5 ml/kg, i.p.) were administered 60 min before the test. In the novel object recognition test, haloperidol (0.1 mg/kg, 5 ml/kg, i.p.) and clozapine (1.0 mg/kg, 5 ml/kg, i.p.) were administered 30 min before the training session. Dosages of the drug were selected based on our previous study.[25]

Behavioral analyses

Behavioral test battery.—Initially, male mice were tested from postnatal week 6 to week 14 with a battery of behavioral paradigms in the following order: locomotion and stereotypy/open field, rotarod, social interaction and novelty, spontaneous T maze alternation, novel object/location recognition, prepulse inhibition, forced swim, tail flick, contextual fear conditioning. The sequence of specific assays spaced by 3–6 days interassay interval was adapted from previously published reports.[26,27] In subsequent antipsychotics studies, mice were tested only once with antipsychotics treatment in only one behavioral assay.

Locomotion and stereotypy assays.—Locomotor activity and stereotypy were performed as described previously.[28] Mice were placed into a locomotion test chamber (40 × 40 cm, Med Associates, Fairfax, VT, USA), and allowed to habituate for 30 min before test. For HAL and CLZ dose response experiments, the habituation step was skipped because of the known effect of both drugs decreasing spontaneous locomotor activity. The horizontal, vertical and stereotypic activities were recorded for 1 h and analyzed by Activity Monitor 5 software (Med Associates).

Social interaction and novelty assay.—The social interaction and novelty assay was performed as described before.[29] The apparatus for the social interaction test comprises a rectangular three-chambered Plexiglas box (manufactured by carpentry facility, University of California, Irvine). Each chamber is 20 × 40 × 20 cm and the dividing walls are made with a movable door in the middle with a 5 cm opening, which allows free access to each chamber. Two empty wire mesh containment cups (9 cm diameter × 10 cm height) were placed in the middle of the right or left chamber (one per each side). The assay consists of a social interaction phase and a social novelty phase. In the social interaction phase, the subject mice were first placed in the middle chamber and allowed to explore for 5 min with the dividing doors closed. A control mouse (an unfamiliar mouse of the same strain, gender and age that had no prior contact with the subject mouse) was placed inside the containment cup that is located in one of the side chambers. The placement of the control mouse in the side chambers was counter-balanced between trials. After habituation, the dividing doors were removed between the compartments to allow free access for the subject mouse to explore the three chambers for 10 min. The duration and number of direct contacts between the subject mice with both cups were recorded individually. Immediately after the social interaction phase, the subject mouse was briefly returned to the middle chamber with dividing doors closed. A second control mouse was then placed inside the containment cup that located in the opposite side chamber. The dividing doors were removed again to allow free access for the subject mouse to explore the three chambers for another 10 min. The duration and number of direct contacts between the subject mice with both cups were recorded individually. Direct contact between the subject mouse and the cup or the body of the subject mouse except for the tails in an area 3 cm around the cup was counted as an active contact. Tests were video recorded and analyzed by ANY-MAZE software (Stoelting, Wood Dale, IL, USA).

Spontaneous T maze alternation assay.—The spontaneous T maze alternation assay was performed as described previously.[30] Mice were placed in the start area of the T maze (main stem: 30 cm long, 12.5 cm wide and 28 cm high; side arms: 15.3 cm long, 13 cm wide and 28 cm high; start area: 8 cm long, 12.5 cm wide, AccuScan Instruments, Columbus, OH, USA) and allowed 30 s of acclimation before the start of each trial. After the acclimation, the sliding door was open and mice were allowed to make a free choice into either side arm. After the choice (all four paws in the chosen arm), the arm sliding door was closed and the mice were allowed to explore the arm for 30 s before being returned to the start area for the next trial. A total of eight trials were completed (seven total possible alternations). Percentage of alternation was calculated as 100 × (number of alternations/7). Time to make a choice was also recorded.

Novel object recognition and location-dependent object recognition assays.—The novel object recognition (NOR) and location-dependent object recognition (LOR) assays were performed as described previously.[31] This task consists of a training phase and a testing phase. Before training, all mice were handled 1–2 min a day for 3 days and were habituated to the experimental apparatus 10 min a day for 3 consecutive days without objects. The experimental apparatus is a rectangular open field (20 × 40 × 20 cm, manufactured by carpentry facility, University of California, Irvine). During the training

phase, mice were placed in the experimental apparatus with two identical objects (for NOR: PVC male pipe adapter, white, 1.5 inch × 2.2 inch; PVC female hose mender, green, 1.4 inch × 2.2 inch; for LOR: shrub spray, black, 1.25 inch × 2.5 inch) and allowed to explore for 10 min. Exploration was defined as occurring when an animal faced an object within one inch or less or when any part of the animal body touched the object, except for the tail. The objects were thoroughly cleaned with 10% ethanol and then dried between trials to make sure no olfactory cues were present. Twenty-four hours later, mice were given the retention test. During NOR retention tests, mice were allowed to explore the experimental apparatus for 5 min in the presence of one familiar and one novel object. The location of the novel object was counterbalanced between trials. Duration and the number of times that the mice explored familiar or novel objects were recorded individually. During LOR retention tests, mice were allowed to explore the experimental apparatus for 5 min in the presence of one familiar object placed in the same location as during the training phase and another familiar object placed in a novel location. The location of the novel object which was placed in the same location as during the training phase was counterbalanced between trials. Duration and the number of times that the mice explored objects placed in familiar or novel location were recorded individually. The relative exploration time was recorded and expressed by a discrimination index: [D.I. = (Tnovel − Tfamiliar)/(Tnovel + Tfamiliar) × 100%]. Tests were video recorded and analyzed by ANY-MAZE software (Stoelting).

Prepulse inhibition assay.—The prepulse inhibition (PPI) assay was measured as previously described.[32] The startle chamber consists of a nonrestrictive Plexiglas cylinder resting on a platform inside of a ventilated and sound attenuated box. A high frequency loudspeaker inside each chamber produced background noise of 65 dB as well as the various acoustic stimuli. Vibrations of the Plexiglas cylinder caused by the body startle response of the animal are converted into analog signals by a piezoelectric accelerometer attached to the platform (San Diego Instrument, San Diego, CA, USA). A total of 65 readings are recorded at 1 millisecond (ms) intervals beginning at the stimulus onset. Average amplitude over this time is used as the measure of startle. Calibration was performed before every use to ensure the accuracy of the sound levels and startle measurements.

During the test, mice were placed in the startle chambers for 5 min acclimation with 65 dB background noise. The PPI session consisted of five different trials: no-stimulus trials, three prepulse trials and startle trials. No-stimulus trials consist of background noise only (65 dB). Startle trials consist of a 40 ms duration startle stimulus at 120 dB (p120). Prepulse trials consist of a 20 ms duration prepulse at 68 dB (pp3), 71 dB (pp6) or 77 dB (pp12), a 100 ms inter-stimulus interval, followed by a 40 ms duration startle stimulus at 120 dB. Test sessions began with five presentations of the p120 trial, followed by 10 presentations of the no-stimulus trial, p120 trials, pp3, pp6 and pp12 prepulse trials given in a pseudorandom order with an inter-trial interval of 8–23 s (mean 15 s) and ending with five presentations of the p120 trial. The amount of PPI is calculated as a percentage score for each acoustic prepulse intensity: %PPI = 100 − ([(startle response for prepulse+pulse trials)/ (startle response for pulse-alone trials)] × 100). The magnitude of the response was calculated as the average response to all of the startle or prepulse trials.

Contextual fear conditioning assay

The contextual fear conditioning assay was performed as previously described.[33] Mice were handled 1 min a day for 3 days before training. For the training session, mice were placed in the conditioning chamber (TSE Systems, Chesterfield, MO, USA) for 2.5 min before receiving a 0.7 mA scrambled foot shock lasting for 2 s. After an additional 30 s in the chamber, mice were returned to their home cages. Freezing behavior was assessed prior to and after the shock (pre- and post-shock sessions) in the chamber, which was defined as the complete lack of movement for at least 3 s in an interval of 5 s. Twenty-four hours after training, mice were placed back into the same chamber (same conditioned context: wall paper with striped pattern) in the absence of shock for 5 min and their freezing behavior was assessed during this period (retention session). Freezing behavior was scored as freezing[1] or not (0) within an interval of 5 s and the percentage of freezing behavior was calculated as 100 × (the number of intervals of freezing/total intervals).

5-Bromodeoxyuridine labeling and immunohistochemistry

5-Bromodeoxyuridine (BrdU) (75 mg/kg, 5 ml/kg, i.p.) was administered to mice to study proliferation and neuronal survival. To investigate proliferation, mice (11 weeks old) received a single dose of BrdU, and were killed 24 h later. To investigate neuronal survival and fate, mice (11 weeks old) received BrdU injections twice with 6 h interval (0900and 1500 hours) at day 0 and were killed 21 days after the last injection of BrdU.

Mice were deeply anesthetized with isofluorane and perfused intracardially with 40 ml ice-cold saline, followed by 50 ml of 4% paraformaldehyde in phosphate-buffered saline (PBS). Brains were then removed, and post-fixed in 4% paraformaldehyde for overnight at 4 °C. Twenty μm coronal sections were cut at the level of the dentate gyrus of the hippocampus.[34] For BrdU labeling, sections were treated with 2N HCl for 30 min. Sections were then blocked with 4% normal goat serum in PBS with 0.3% Triton X-100 for 60 min, and then incubated with the primary antibodies (anti-BrdU, 1:500, Thermo Fisher, Hampton, NH, USA; antidoublecortin (anti-DCX), 1:500, Aves, Tigard, OR, USA; anti-glial fibrillary acidic protein (anti-GFAP), 1:500, Aves; anti-NeuN, 1:500, Abcam, Cambridge, MA, USA) for 24 h at room temperature. After three wash-steps with PBS, sections were incubated with goat Alexa Fluor 568 anti-mouse (1:500, Life Technologies, Carlsbad, CA, USA) and 4′,6-diamidino-2-phenylindole (DAPI) for 1 h at room temperature. Sections were then washed with PBS three times and mounted with anti-fade solution. After staining, slides were analyzed using Zeiss microscope (Carl Zeiss, Thornwood, NY, USA), and Zeiss LSM image browser software (Carl Zeiss) was used for image acquisition and analysis. The number of $BrdU^+$ cells was counted on sections.

For BrdU staining, we counted $BrdU^+$ cells in all sections in the levels (Bregma − 1.58 to − 2.30). To determine the precise level of sections, an overlay of a mouse brain atlas outline was performed using Transparent Image Overlay program (https://imagej.nih.gov/ij/plugins/image-overlay/). If a section is damaged in one animal, the sections at the same levels from other animals were excluded. AxioVision software (Zeiss Microscopy, Thornwood, NY, USA) was used to measure the surface of each dentate gyrus, and the sizes were then normalized. For double-immunostaining of DCX, NeuN and GFAP with BrdU, every one

out of four hippocampus sections was immunostained. Cell counting was carried out by observers who were blinded to the treatment and unfamiliar with the experiment conditions.

mRNA microarray analysis

We performed microarray experiments and analysis as previously described.[35] Whole brain tissues were dissected from male mice. Total RNA was extracted (Qiagen, Germantown, MD, USA) according to the manufacturer's protocol. RNA samples with A260/A280 absorbance ratios between 2.00 and 2.20 were reverse-transcribed into cDNA and analyzed by 'whole-transcript transcriptomics' using the GeneAtlas microarray system (Affymetrix, Santa Clara, CA, USA) and the manufacturer's protocols.

MoGene 1.1 ST array strips (Affymetrix) were used to hybridize to newly synthesized sscDNA.

Each array comprised 770 317 distinct 25-mer probes to probe an estimated 28 853 transcripts, with a median 27 probes per gene.

Gene expression changes associated with the methionine treatment were analyzed with transcriptome analysis console software (Affymetrix) using Tikey's Bi-weight Average algorithm and default settings, generating fold-change and unpaired ANOVA values, reported in Supplementary Tables S1.1 and S1.2. Gene expression changes did not reach $P<0.05$ after Benjamini-Hochberg step-up false discovery rate procedure to correct for multiple comparisons, given the relatively small number of samples and large number of genes tested. However, gene expression changes uncovered using the initial microarray screen were subsequently validated using real-time qPCR in the same samples (see Figures 4c–g).

Quantitative real-time PCR

Whole brain, hippocampal and cortical tissues were dissected from male mice. mRNA was extracted (Qiagen) and reverse-transcribed (Thermo Fisher) following the manufacturer's instructions. RT-qPCR was performed using SYBR Green reagents (Life Techonologies), and analyzed by ABI 7000 sequence detection system (Applied Biosystems, Foster City, CA, USA) with gene-specific primers as previously reported.[36] Three to four animals per treatment group were used for analysis of the whole brain mRNA. For the subregional analysis, 6–7 animals were used. For each sample, GAPDH was used as an internal control. For each target gene sample, the relative abundance value obtained for the reference gene was divided by the value derived from the control sequence in the corresponding target gene. Values were calculated using the following equation: $= 2^{(CT(target,untreated) - CT(ref,untreated)) - (CT(target,treated) - CT(ref,treated))}$.

The following primers were used:

EGR2-For: 5′-GTCACCTCCGCCTCCCCCAACC-3′

EGR2-Rev: 3′-GGCGGCGATAAGAATGCTGAAGGA-5′

ARC-For: 5′-GGAGTCCATGGGCGGCAAATAC-3′

ARC-Rev: 3′-GCGGCAGGTGGCGGGGTGATG-5′

NPAS4-For: 5′-GTCTTGCCTGCATCTACACTCG-3′

NPAS4-Rev: 3′-TGGCCCAGATGCTCGCTCACACT-5′

FOS-For: 5′-TGAGGCTTCCACCCCAGAGTC-3′

FOS-Rev: 3′- AACTACTGAAGAACAAAGGCCGT-5′

FGF1-For: 5′-GCAACGGGGGCCACTTCTT-3′

FGF1-Rev: 3′-ATATACACTTCGCCCGCACTTTC-5′

GAPDH-For: 5′-TGGCACAGTCAAGGCTGAGA-3′

GAPDH-Rev: 3′-CGCTCCTGGAAGATGGTGAT-5′

Electrophysiology and laser scanning photostimulation

Horizontal hippocampal slices of 400 μm thick were cut at the angle optimized to conserve the intrahippocampal axonal projections in ice-cold sucrose-containing cutting solution (in mM: 85 NaCl, 75 sucrose, 2.5 KCl, 25 glucose, 1.25 NaH_2PO_4, 4 $MgCl_2$, 0.5 $CaCl_2$ and 24 $NaHCO_3$). Two morphologically intact slices intermediate between dorsal and ventral hippocampus from each animal were used for experiments. Slices were first incubated in sucrose-containing artificial cerebrospinal fluid (ACSF) for 30 min–1 h at 32 °C, and then transferred to recording ACSF (in mM: 126 NaCl, 2.5 KCl, 26 $NaHCO_3$, 2 $CaCl_2$, 2 $MgCl_2$, 1.25 NaH_2PO_4 and 10 glucose). Throughout the cutting, incubation and recording, the solutions were continuously supplied with 95% O_2–5% CO_2. Our overall system of electrophysiological recording, photostimulation and imaging was described previously.[37,38] For laser scanning photostimulation experiments, the microscope objective was switched from × 60 to × 4. Stock solution of MNI-caged- L-glutamate (Tocris Bioscience, Pittsburgh, PA, USA) was added to 20 ml of ACSF for a concentration of 0.2 mM caged glutamate. The slice image was acquired by a high resolution digital CCD camera, which in turn was used for guiding and registering photostimulation sites. During mapping experiments, photostimulation was usually applied to 16 × 16 patterned sites (with an inter-site space of 100 μm^2) covering the whole hippocampus in a nonraster, nonrandom sequence to avoid revisiting the vicinity of recently stimulated sites. Whole-cell voltage-clamp recordings were made from the recorded neurons to measure photostimulation-evoked excitatory postsynaptic current responses at the holding potential around − 70 mV, which was based upon the empirically determined GABAergic reversal potentials at the recorded mouse ages. Photostimulation data analysis has been described in detail.[39]

Human studies

We screened publically available gene expression studies in the context of schizophrenia to obtain human gene expression data. The most comprehensive repositories of such data, Gene Expression Omnibus and ArrayExpress, returned 10 studies with differential gene expression (RNA microarray) data from individuals with schizophrenia and healthy controls.

Only curated GEO data sets that feature in NCBI's GDSbrowser and contain gene expression information from the prefrontal cortex in the brain were included, in order to maintain comparability with our mouse data. Additionally, differential NPAS4 expression uncovered by the probe set '1554299_at' was deemed reliable based on the annotation grade (A) given by NetAffx (Affymetrix). These selection steps narrowed down the number of usable data sets to just one; GDS4523, which included post-mortem tissue samples from the anterior prefrontal cortex (Brodmann Area 10) of schizophrenic patients and healthy controls.[40] The latter data set provided gene expression data from 27 cases (schizophrenia) and 22 matched controls, of these 18 were male patients and 11 were male controls. Mean age (years) and post-mortem delay (hours) values for cases and controls were registered. These values were fairly matched between cases and controls; mean ages were 73.3 and 69 for schizophrenia patients and controls, respectively, while mean post-mortem delay is 8.1 and 9.4 for schizophrenia patients and controls, respectively. One sample (GSM439786) from GDS4523 was excluded as it was deemed an outlier with an expression value that exceeded the average for all other samples by 2400-fold.

Data analysis

Animal studies: GraphPad Prism (GraphPad Software, La Jolla, CA, USA) was used for statistical analysis. Data are presented as means ± s.e.m. Results were analyzed by student t-test or ANOVA followed by the appropriate *post hoc* comparisons, and $P<0.05$ was considered statistically significant. We have used peer-reviewed literature for each of the behavioral experiments to estimate the minimum number of animals required to obtain statistically significant results. Statistical calculations take into account these sample sizes when determining an overall significant effect.

Human study: differential expression between patients and controls was computed using empirical Bayes moderated t-statistics test performed by the limma R package.

RESULTS

Pregnant mice were administered L-methionine (750 mg/kg) or saline twice a day for 7 to 8 consecutive days from gestational day 14 until delivery. This dose is equivalent to twice their regular dietary methionine intake, effectively tripling their methionine intake. The treatment did not affect the dam weight, food intake and pregnancy duration; neither did it affect the number of the progeny or the gender ratio (data not shown).

When compared to the offspring of saline-injected dams (SAL mice), the offspring of methionine-injected dams (MET mice) appeared healthy and were of normal bodyweight throughout their entire growth period ($P>0.05$, Supplementary Figures S2a and b). Furthermore, the MET mice traveled similar distances in the center area in the open-field assay ($P>0.05$, Supplementary Figure S2a), displayed similar motor coordination in the rotarod assay ($P>0.05$, Supplementary Figure S2b), similar nociceptive responsiveness in the tail flick assay ($P>0.05$, Supplementary Figure S2c), and similar immobility time in the forced swim assay, ($P>0.05$, Supplementary Figure S2d).

MET mice display selective behavioral deficits and impairments that mimic a schizophrenia phenotype

In contrast, MET mice exhibited a twofold increase in their horizontal and vertical locomotor activities, indicated by the increase in total distance traveled and vertical counts ($P<0.05$, Figures 1b and c). They also displayed increased stereotypic behaviors ($P<0.01$, Figure 1d).

In the social interaction assay, MET mice displayed less interaction with the unfamiliar mice ($P>0.05$, Figure 1e) than did the SAL group ($P<0.001$, Figure 1e). In the second (social novelty) phase, MET mice displayed less interaction with the new, unfamiliar mice ($P>0.05$, Figure 1f) than did those in the SAL group ($P<0.05$, Figure 1f). Thus, MET mice exhibit impaired sociability and social recognition.

We next compared the MET mice responses in sensorimotor gating behavior. MET mice exhibited a significant increase in their startle reactivity ($P<0.05$, Figure 1g), and significantly decreased PPI ratios ($P<0.05$, Figures 1h and i), compared to SAL mice, suggesting an impairment in sensorimotor gating function. In the novel object recognition assay, both groups spent more time exploring the new object than the old object ($P<0.01$, Figure 1j), but the MET mice showed a decreased discrimination index compared to SAL mice ($P<0.001$, Figure 1k). In the location-dependent recognition assay, unlike SAL mice, MET mice did not discriminate between the objects in the old and new locations ($P>0.05$, Figures 1l; $P<0.001$, Figure 1m). We further evaluated these animals in two other spatial memory-related paradigms. In the contextual fear conditioning assay, both groups exhibited similar levels of freezing behavior during the training and stimulus session ($P>0.05$, Figure 1n). In the retention session, however, MET mice exhibited a decrease in the freezing behavior percentage ($P<0.01$, Figure 1n). In the spontaneous T maze alternation assay, MET mice also showed a decrease in the percentage of arm choice alternation ($P<0.01$, Figure 1o). Together, these results suggest that MET mice display cognitive deficits, in particular as they relate to spatial learning and memory function.

MET mice display abnormal brain weight, reduced neurogenesis and increased gliogenesis

Although MET mice display no changes in body weight, the weight of their brains was found to be slightly lower in both the absolute value and the brain/body weight ratio ($P<0.05$, Supplementary Figures S3a and b).

Immunohistology revealed a decrease in the number of $BrdU^+$ cells in the subgranular zone of the hippocampal dentate of MET group (34.7 ± 2.3 cells/mm^2) compared with the SAL group (46.6 ± 2.9 cells/mm^2) 24 h after BrdU injection ($P<0.05$, Figures 2b and f), suggesting that elevated methionine causes a decrease in cell proliferation of neural stem cells.

To evaluate the survival and the fate of newborn neurons, $BrdU^+$ cells were examined over a 21-day period after two BrdU injections (21-day-old $BrdU^+$ cells). The number of 21-day-old $BrdU^+$ cells in MET mice was ~40% lower than in SAL mice ($P<0.01$, Figure 2g). In addition, there was a considerable decrease in the proportion of $BrdU^+$ cells that co-stained

for DCX in MET mice (18.2 ± 3.5%) versus SAL mice (38.1 ± 3.5%, $P<0.05$, Figures 2c and h), and in the proportion of $BrdU^+$ cells that co-stained for NeuN in MET mice (85.98 ± 2.2%) versus SAL mice (56.17 ± 7.6%, $P<0.05$, Figures 2d and i). Conversely, a higher percentage of $BrdU^+$ cells that co-stained as $GFAP^+$ astrocytes were observed in MET mice (22.1 ± 5.2%) than in SAL mice (5.3 ± 1.2%, $P<0.05$, Figures 2e and j). These results suggest that the methionine treatment suppresses adult hippocampal neurogenesis, by modulating the proliferation and differentiation of neural stem cells.

MET mice exhibit reduced local excitatory synaptic connections of the CA1 excitatory pyramidal neurons

We investigated whether the prenatal treatment affects synaptic connectivity in the hippocampus, in particular the CA1 region, by applying the laser scanning photostimulation approach, which is used for effective and detailed local circuit mapping. We show that the photostimulation responses of the recorded CA1 pyramidal neurons (exemplar somatic locations indicated as the red circles in Figures 3a and b for SAL group and in Figures 3d and e for MET mice) to direct uncaged glutamate activation are significantly weaker in MET mice than SAL mice, (see red traces in Figure 3c versus Figure 3f). Quantitative analysis of the direct uncaging responses for both groups shows a significant reduction for MET mice ($P<0.01$, Figure 3g). In addition, we show that the intrinsic membrane excitability of the CA1 neurons MET group was unaffected (P>0.05, Figure 3h). These data suggest that the CA1 excitatory pyramidal neurons in the MET mice have reduced local excitatory synaptic connections.

MET mice exhibit downregulation of neuronal immediate early genes

To determine which genes' expression are affected in the MET mice, we carried out a global brain mRNA microarray analysis covering 28 853 genes (Figures 4a and b). We found 122 genes displaying changes in expression (with a 41.2-fold change, shown in Supplementary Tables S1.1 and S1.2). Among the subset of genes that exhibited a ≥ 1.5-fold change ($P<0.05$, Supplementary Tables S1.1 and S1.2) was a set of four neuronal immediate early genes and a growth factor. Npas4, Arc, Dusp1, c-Fos and Egr2 were downregulated, while *Fgf1* was upregulated. Results of quantitative real-time PCR confirmed our microarray findings ($P<0.01$, <0.05, <0.01, <0.05, >0.05 for *Npas4, Arc, Egr2, Fos* and *Fgf1*, respectively, Figures 4c-g). Using arbitrary fold change (FC) cutoffs of ≥ 2 and significance *P*-values of <0.01, only *Npas4* showed a significant change (a decrease by 2.37-fold in MET versus SAL offspring, $P = 0007$) in whole brain tissues (Supplementary Tables S1.1 and S1.2). We then analyzed using quantitative real-time PCR the differential gene expression of Npas4 in the prefrontal cortex and hippocampus. The results reveal 4twofold decreases in mRNA levels only in the MET mice prefrontal cortex ($P<0.05$, Figure 4h) and hippocampus ($P>0.05$, Figure 4i), respectively.

NPAS4 is downregulated in prefrontal cortex of post-mortem schizophrenia patients

Because the MET mice exhibit behavioral abnormalities that mimic schizophrenia symptoms,[41] we analyzed Npas4 gene expression in samples from schizophrenia patients. The expression of Npas4 in the BA10 region from individuals with schizophrenia was significantly reduced in comparison with healthy controls. Maleonly data from the data set

GDS4523 indicate that Npas4 downregulation is highly statistically significant, P=0.007 and LogFC = − 1.139, Figure 4j). A similar trend was noted when male and female data were both included in the analysis; P = 0.0189 and LogFC = − 0.733, Figure 4k).

Antipsychotics differentially restore the behavioral deficits of the prenatal methionine-induced phenotype

Because the MET mice displayed behavioral phenotypes and biochemical changes that resemble schizophrenia-like symptoms, we investigated the effects of two antipsychotic drugs on these behaviors, choosing haloperidol and clozapine as representative of typical and atypical antipsychotics, respectively. We found that a single injection of haloperidol (0.1 mg/kg) or clozapine (1.0 mg/kg) reversed the locomotor hyperactivity and stereotypic behavior of the MET mice (P<0.01, Figures 5a and b). While both haloperidol (0.1 mg/kg) and clozapine (1.0 mg/kg) failed to reverse the social novelty deficit of the MET mice (P>0.05, Figure 5d), only clozapine was able to reverse their social withdrawal symptom (P<0.05, Figure 5c). Haloperidol (0.25 mg/kg) or clozapine (2.5 mg/kg) reversed PPI deficits in Met mice, although their average PPI ratios were also not statistically different from those of the SAL mice (P>0.05, Figure 5e). In the novel object recognition assay, clozapine (1.0 mg/kg) but not haloperidol (0.1 mg/kg) was able to reverse the object recognition deficit (P<0.001, Figure 5f). The discrimination index of the clozapine-treated group was similar to those of both the SAL and the MET mice (P>0.05, Figure 5g).

DISCUSSION

Multiple prior lines of evidence suggested the methionine cycle as a potentially important player in the etiology of schizophrenia. Since schizophrenia is a developmental disorder, we investigated what effect perturbation of the methionine cycle during late pregnancy would have on progeny behavior. We found that MET mice display behavioral deficits highly reminiscent of human schizophrenia. MET mouse brains also exhibited abnormally reduced local excitatory synaptic connections, and a statistically highly significant ≥ twofold downregulation in neural Npas4 expression that was recapitulated in the brains of human schizophrenics.

Npas4 promotes GABA-mediated inhibitory transmission during development, and regulates the maintenance of inhibitory synapses in response to excitatory synaptic activity.[42–44] *Npas4* is also known to regulate a mechanism that underlies memory formation.[45] Indeed, *Npas4* regulates transcriptional programs involving several other neuronal activity-regulated immediate early genes such as *Arc, c-Fos* and *Egr2*, which also play important roles in synaptic plasticity and cognitive functions.[46–49] Interestingly, mice deficient in *Npas4* display a behavioral phenotype that is strikingly similar to that which we observed in MET mice.[50] Knockdown of *Npas4* expression in mouse embryonic stem cells undergoing neural differentiation inhibits their ability to differentiate appropriately, and results in delayed neural differentiation.[51] *Npas4* downregulation in MET mice might be a mechanism for the decreased neurogenesis and delayed differentiation of embryonic stem cells, as well as the cognitive impairment in these animals. The regional differential expression analysis of

Npas4 expression in MET mice' brains shows a decrease in the prefrontal cortex and a similar decrease (albeit not statistically significant) in the hippocampus.

Disruptions of excitatory and inhibitory synaptic transmissions and plasticity may play a role in cognitive impairments, and are steadily being implicated in the major psychiatric disorders, such as autism, schizophrenia, bipolar disorder, social anxiety, attention-deficit hyperactivity disorder and Alzheimer's disease.[52–56] Therefore, factors such as methionine administration during pregnancy that cause dysregulation of *Npas4* expression may increase the risk of neuropsychiatric disorders. This, together with our transcriptomic data from MET mice, led us to investigate whether *Npas4* expression is altered in the brain of schizophrenia patients. Differential gene expression data from the data set that was fit for inclusion (GDS4523) revealed the downregulation of *Npas4* in the region BA10 in schizophrenia patients, as evidenced by the highly significant *P*-value for male patients. The level of significance was reduced by including female patients in the analysis; nevertheless, the reduction in *Npas4* expression remained significant in schizophrenia BA10 samples compared to their healthy counterparts. The downregulation of *Npas4* in the prefrontal cortex of post-mortem patients with schizophrenia strongly supports a role for this gene in the etiology of schizophrenia. Clearly, further experimental validation of this particular trend is necessary. Despite the fact that studied schizophrenia patients were exposed to antipsychotic medications, which may affect *Npas4* expression, the results lend strong support to the here-reported findings pertaining to *Npas4* expression in the mouse model.

The correlation between the biochemical and behavioral data of the MET pups and the corresponding data known for schizophrenia led us to test whether antipsychotics can reverse the behavioral deficits of the MET mice. We tested the typical (haloperidol) and atypical (clozapine) antipsychotic drugs on the behavioral responses of the MET pups. Both typical and atypical antipsychotics were able to reverse stereotypy and hyperlocomotor activity, but only the atypical antipsychotic (clozapine) could improve the deficits in novel object recognition and social interaction. Our findings concur with data in the clinical literature that support the cognitive efficacy of the atypical antipsychotics.[57–60] However, the human analogs of our findings should be treated with caution for two reasons. First, animal studies are not always comparable to clinical studies, particularly when assessing cognition. Second, there is still unresolved debate on the efficacy of atypical antipsychotics to treat cognitive impairment and negative symptoms in schizophrenia,[57–61] for review see ref. 62.

Impairments in cognitive function are observed across the major neuropsychiatric disorders.[63,64] Based on our results, we propose that prenatal methionine is a critical factor for programming the expression of key neuronal activity-regulated genes and neuronal plasticity, and that perturbed methionine metabolism during gestation results in dysregulation of these genes and a number of developmental abnormalities collectively linked with a behavioral phenotype that mirrors schizophrenia.[65–67] In this respect, a recent study has indicated that methionine intake during developmental, but not adulthood, stage increases global DNA methylation and decreases gabrb2 promoter methylation associated with a significant increase in gabrb2 mRNA levels in zebrafish.[68]

Our study provides insight into the long-term developmental effects of prenatal disruption of the one-carbon metabolism, but carries a number of limitations. First, folate, homocysteine and methylation were not quantified and their relation to phenotypes was not verified, and therefore, we cannot conclude whether methionine itself or its downstream effects are responsible for the deficits. Second, sex differences may also play a role and need to be investigated. These questions are important and they are the focus of our ongoing work. In addition, our results could be viewed as inconsistent with a number of clinical studies that show folate deficiency,[69,70] and its beneficial effects in schizophrenic patients,[71] the beneficial effects of early gestational folate exposure on subsequent schizophrenia[72] and autism[65] risk, as well as the detrimental effects of famine on subsequent schizophrenia risk.[66–68,73] However, while too little folic acid is known to result in damages associated with neural tube defects[74] and with schizophrenia,[22] animal studies demonstrate that too much folic acid during pregnancy may result in embryonic growth delay, and memory impairment.[75] This suggests that imbalances in the one-carbon metabolism can have differential adverse effects depending on the metabolites' concentrations. More studies are necessary to resolve the differences between the animal models and the clinical data.

Our results have significant clinical implications. It is important to note that in humans, one-carbon homeostasis during gestation is finely regulated by the interaction between environmental factors (dietary methionine, B12 and folate, and the balance of methionine and other amino acids) and genetic factors (polymorphisms in onecarbon-metabolism-related genes).[69–71] While methyl-donor nutrients determine the availability of methyl groups, gene polymorphisms of methionine-cycle enzymes determine utilization of the dietary methyl-group. Human dietary methionine intake has dramatically increased in the past few decades.[76] In pregnant women, this may carry special risks, considering the alterations in methyl-donor requirements and methionine metabolism during the different gestation and developmental stages. Further studies are needed to determine gene-nutrient interactions in the risk of schizophrenia, and to define the upper safe level of methionine intake during pregnancy. In addition, MET mice constitute a valuable model for investigating the precise mechanistic connections between environmental and genetic factors implicated in neuropsychiatric disorders.

In conclusion, our data show that methionine administration during pregnancy result in profound biochemical and gene expression changes as well as in the behavior of the progeny. MET mice display schizophrenia-like deficits that are reversed by antipsychotics. The one-carbon metabolism pathway may, therefore, represent a potentially exciting therapeutic target for in antipsychotic drug development.

Supplementary Material

Refer to Web version on PubMed Central for supplementary material.

ACKNOWLEDGMENTS

This work was supported by the National Institute of Health (DA024746), CART and Eric L and Lila D Nelson Chair in Neuropharmacology. AA is supported by the Institute of International Education IIE-SRF fellowship.

REFERENCES

1. Loenen WA. S-adenosylmethionine: jack of all trades and master of everything? Biochem Soc Trans 2006; 34(Pt 2): 330–333. [PubMed: 16545107]
2. Kim M, Park YK, Kang TW, Lee SH, Rhee YH, Park JL et al. Dynamic changes in DNA methylation and hydroxymethylation when hES cells undergo differentiation toward a neuronal lineage. Hum Mol Genet 2014; 23: 657–667. [PubMed: 24087792]
3. Chen Y, Ozturk NC, Zhou FC. DNA methylation program in developing hippo-campus and its alteration by alcohol. PLoS ONE 2013; 8: e60503. [PubMed: 23544149]
4. Horvath S, Zhang Y, Langfelder P, Kahn RS, Boks MP, van Eijk K et al. Aging effects on DNA methylation modules in human brain and blood tissue. Genome Biol 2012; 13: R97. [PubMed: 23034122]
5. Wu H, Coskun V, Tao J, Xie W, Ge W, Yoshikawa K et al. Dnmt3a-dependent nonpromoter DNA methylation facilitates transcription of neurogenic genes. Science 2010; 329: 444–448. [PubMed: 20651149]
6. Krebs MO, Bellon A, Mainguy G, Jay TM, Frieling H. One-carbon metabolism and schizophrenia: current challenges and future directions. Trends Mol Med 2009; 15: 562–570. [PubMed: 19896901]
7. Pollin W, Cardon PV, Jr, Kety SS. Effects of amino acid feedings in schizophrenic patients treated with iproniazid. Science 1961; 133: 104–105. [PubMed: 13736870]
8. Antun FT, Burnett GB, Cooper AJ, Daly RJ, Smythies JR, Zealley AK. The effects of L-methionine (without MAOI) in schizophrenia. J Psychiatr Res 1971; 8: 63–71. [PubMed: 4932991]
9. Osmond H, Smythies J. Schizophrenia: a new approach. J Ment Sci 1952; 98: 309–315. [PubMed: 14917992]
10. Hei G, Pang L, Chen X, Zhang W, Zhu Q, Lu L et al. Association of serum folic acid and homocysteine levels and 5, 10-methylenetetrahydrofolate reductase gene polymorphism with schizophrenia. Zhonghua Yi Xue Za Zhi 2014; 94: 2897–2901. [PubMed: 25549641]
11. Kale A, Naphade N, Sapkale S, Kamaraju M, Pillai A, Joshi S et al. Reduced folic acid, vitamin B12 and docosahexaenoic acid and increased homocysteine and cortisol in never-medicated schizophrenia patients: implications for altered one-carbon metabolism. Psychiatry Res 2010; 175: 47–53. [PubMed: 19969375]
12. Hu CY, Qian ZZ, Gong FF, Lu SS, Feng F, Wu YL et al. Methylenetetrahydrofolate reductase (MTHFR) polymorphism susceptibility to schizophrenia and bipolar disorder: an updated meta-analysis. J Neural Transm 2014; 122: 307–320. [PubMed: 24938371]
13. Jadavji NM, Bahous RH, Deng L, Malysheva O, Grand'maison M, Bedell BJ et al. Mouse model for deficiency of methionine synthase reductase exhibits short-term memory impairment and disturbances in brain choline metabolism. Biochem J 2014; 461: 205–212. [PubMed: 24800750]
14. Nohesara S, Ghadirivasfi M, Mostafavi S, Eskandari MR, Ahmadkhaniha H, Thiagalingam S et al. DNA hypomethylation of MB-COMT promoter in the DNA derived from saliva in schizophrenia and bipolar disorder. J Psychiatr Res 2011; 45: 1432–1438. [PubMed: 21820670]
15. Roffman JL, Weiss AP, Deckersbach T, Freudenreich O, Henderson DC, Wong DH et al. Interactive effects of COMT Val108/158Met and MTHFR C677T on executive function in schizophrenia. Am J Med Genet B Neuropsychiatr Genet 2008; 147B: 990–995. [PubMed: 18186041]
16. Lajin B, Alhaj Sakur A, Michati R, Alachkar A. Association between MTHFR C677T and A1298C, and MTRR A66G polymorphisms and susceptibility to schizophrenia in a Syrian study cohort. Asian J Psychiatry 2012; 5: 144–149.
17. Roffman JL, Brohawn DG, Nitenson AZ, Macklin EA, Smoller JW, Goff DC. Genetic variation throughout the folate metabolic pathway influences negative symptom severity in schizophrenia. Schizophr Bull 2013; 39: 330–338. [PubMed: 22021659]
18. Saradalekshmi KR, Neetha NV, Sathyan S, Nair IV, Nair CM, Banerjee M. DNA methyl transferase (DNMT) gene polymorphisms could be a primary event in epigenetic susceptibility to schizophrenia. PLoS ONE 2014; 9: e98182. [PubMed: 24859147]

19. Cordero P, Milagro FI, Campion J, Martinez JA. Maternal methyl donors supplementation during lactation prevents the hyperhomocysteinemia induced by a high-fat-sucrose intake by dams. Int J Mol Sci 2013; 14: 24422–24437. [PubMed: 24351826]
20. Dominguez-Salas P, Moore SE, Baker MS, Bergen AW, Cox SE, Dyer RA et al. Maternal nutrition at conception modulates DNA methylation of human metastable epialleles. Nat Commun 2014; 5: 3746. [PubMed: 24781383]
21. Xu J, He G, Zhu J, Zhou X St, Clair D, Wang T et al. Prenatal nutritional deficiency reprogrammed postnatal gene expression in mammal brains: implications for schizophrenia. Int J Neuropsychopharmacol 2014; 18.
22. Picker JD, Coyle JT. Do maternal folate and homocysteine levels play a role in neurodevelopmental processes that increase risk for schizophrenia? Harv Rev Psychiatry 2005; 13: 197–205. [PubMed: 16126606]
23. Waterland RA, Kellermayer R, Laritsky E, Rayco-Solon P, Harris RA, Travisano M et al. Season of conception in rural gambia affects DNA methylation at putative human metastable epialleles. PLoS Genet 2010; 6: e1001252. [PubMed: 21203497]
24. Brown AS, Bottiglieri T, Schaefer CA, Quesenberry CP, Jr, Liu L, Bresnahan M et al. Elevated prenatal homocysteine levels as a risk factor for schizophrenia. Arch Gen Psychiatry 2007; 64: 31–39. [PubMed: 17199052]
25. Wang L, Alachkar A, Sanathara N, Belluzzi JD, Wang Z, Civelli O. A methionine-induced animal model of schizophrenia: face and predictive validity. Int J Neuropsychopharmacol 2015; 18.
26. Paylor R, Spencer CM, Yuva-Paylor LA, Pieke-Dahl S. The use of behavioral test batteries, II: effect of test interval. Physiol Behav 2006; 87: 95–102. [PubMed: 16197969]
27. McIlwain KL, Merriweather MY, Yuva-Paylor LA, Paylor R. The use of behavioral test batteries: effects of training history. Physiol Behav 2001; 73: 705–717. [PubMed: 11566205]
28. McNamara RK, Logue A, Stanford K, Xu M, Zhang J, Richtand NM. Dose-response analysis of locomotor activity and stereotypy in dopamine D3 receptor mutant mice following acute amphetamine. Synapse 2006; 60: 399–405. [PubMed: 16856172]
29. Kaidanovich-Beilin O, Lipina T, Vukobradovic I, Roder J, Woodgett JR. Assessment of social interaction behaviors. J Vis Exp 2011.
30. Risbrough V, Ji B, Hauger R, Zhou X. Generation and characterization of humanized mice carrying COMT158 Met/Val alleles. Neuropsychopharmacology 2014; 39: 1823–1832. [PubMed: 24509724]
31. McQuown SC, Barrett RM, Matheos DP, Post RJ, Rogge GA, Alenghat T et al. HDAC3 is a critical negative regulator of long-term memory formation. J Neurosci 2011; 31: 764–774. [PubMed: 21228185]
32. Duangdao DM, Clark SD, Okamura N, Reinscheid RK. Behavioral phenotyping of neuropeptide S receptor knockout mice. Behav Brain Res 2009; 205: 1–9. [PubMed: 19646487]
33. Errico F, Rossi S, Napolitano F, Catuogno V, Topo E, Fisone G et al. D-aspartate prevents corticostriatal long-term depression and attenuates schizophrenia-like symptoms induced by amphetamine and MK-801. J Neurosci 2008; 28: 10404–10414. [PubMed: 18842900]
34. Paxinos G KF. The Mouse Brain in Stereotaxic Coordinates. Academic Press: London, UK, 2001.
35. Heerdt PM, Kant R, Hu Z, Kanda VA, Christini DJ, Malhotra JK et al. Transcriptomic analysis reveals atrial KCNE1 down-regulation following lung lobectomy. J Mol Cell Cardiol 2012; 53: 350–353. [PubMed: 22641150]
36. Nagasaki H, Wang Z, Jackson VR, Lin S, Nothacker HP, Civelli O. Differential expression of the thyrostimulin subunits, glycoprotein alpha2 and beta5 in the rat pituitary. J Mol Endocrinol 2006; 37: 39–50. [PubMed: 16901922]
37. San Antonio A, Liban K, Ikrar T, Tsyganovskiy E, Xu X. Distinct physiological and developmental properties of hippocampal CA2 subfield revealed by using anti-Purkinje cell protein 4 (PCP4) immunostaining. J Comp Neurol 2014; 522: 1333–1354. [PubMed: 24166578]
38. Xu X, Roby KD, Callaway EM. Immunochemical characterization of inhibitory mouse cortical neurons: three chemically distinct classes of inhibitory cells. J Comp Neurol 2010; 518: 389–404. [PubMed: 19950390]

39. Shi Y, Nenadic Z, Xu X. Novel use of matched filtering for synaptic event detection and extraction. PLoS ONE 2010; 5: e15517. [PubMed: 21124805]
40. Maycox PR, Kelly F, Taylor A, Bates S, Reid J, Logendra R et al. Analysis of gene expression in two large schizophrenia cohorts identifies multiple changes associated with nerve terminal function. Mol Psychiatry 2009; 14: 1083–1094. [PubMed: 19255580]
41. Carpenter WT, Jr., Buchanan RW, Kirkpatrick B, Tamminga C, Wood F. Strong inference, theory testing, and the neuroanatomy of schizophrenia. Arch Gen Psychiatry 1993; 50: 825–831. [PubMed: 8215806]
42. Bloodgood BL, Sharma N, Browne HA, Trepman AZ, Greenberg ME. The activity-dependent transcription factor NPAS4 regulates domain-specific inhibition. Nature 2013; 503: 121–125. [PubMed: 24201284]
43. Spiegel I, Mardinly AR, Gabel HW, Bazinet JE, Couch CH, Tzeng CP et al. Npas4 regulates excitatory-inhibitory balance within neural circuits through cell-type-specific gene programs. Cell 2014; 157: 1216–1229. [PubMed: 24855953]
44. Maya-Vetencourt JF. Activity-dependent NPAS4 expression and the regulation of gene programs underlying plasticity in the central nervous system. Neural Plast 2013; 2013: 683909. [PubMed: 24024041]
45. Ramamoorthi K, Fropf R, Belfort GM, Fitzmaurice HL, McKinney RM, Neve RL et al. Npas4 regulates a transcriptional program in CA3 required for contextual memory formation. Science 2011; 334: 1669–1675. [PubMed: 22194569]
46. Alberini CM. Transcription factors in long-term memory and synaptic plasticity. Physiol Rev 2009; 89: 121–145. [PubMed: 19126756]
47. Chowdhury S, Shepherd JD, Okuno H, Lyford G, Petralia RS, Plath N et al. Arc/ Arg3.1 interacts with the endocytic machinery to regulate AMPA receptor trafficking. Neuron 2006; 52: 445–459. [PubMed: 17088211]
48. Plath N, Ohana O, Dammermann B, Errington ML, Schmitz D, Gross C et al. Arc/ Arg3.1 is essential for the consolidation of synaptic plasticity and memories. Neuron 2006; 52: 437–444. [PubMed: 17088210]
49. West AE, Greenberg ME. Neuronal activity-regulated gene transcription in synapse development and cognitive function. Cold Spring Harb Perspect in Biol 2011; 3: a005744. [PubMed: 21555405]
50. Coutellier L, Beraki S, Ardestani PM, Saw NL, Shamloo M. Npas4: a neuronal transcription factor with a key role in social and cognitive functions relevant to developmental disorders. PLoS ONE 2012; 7: e46604. [PubMed: 23029555]
51. Klaric TS, Thomas PQ, Dottori M, Leong WK, Koblar SA, Lewis MD. A reduction in Npas4 expression results in delayed neural differentiation of mouse embryonic stem cells. Stem Cell Res Ther 2014; 5: 64. [PubMed: 24887558]
52. Toro R, Konyukh M, Delorme R, Leblond C, Chaste P, Fauchereau F et al. Key role for gene dosage and synaptic homeostasis in autism spectrum disorders. Trends Genet 2010; 26: 363–372. [PubMed: 20609491]
53. Auerbach BD, Osterweil EK, Bear MF. Mutations causing syndromic autism define an axis of synaptic pathophysiology. Nature 2011; 480: 63–68. [PubMed: 22113615]
54. Grant SG. Synaptopathies: diseases of the synaptome. Curr Opin Neurobiol 2012; 22: 522–529. [PubMed: 22409856]
55. Gkogkas CG, Khoutorsky A, Ran I, Rampakakis E, Nevarko T, Weatherill DB et al. Autism-related deficits via dysregulated eIF4E-dependent translational control. Nature 2013; 493: 371–377. [PubMed: 23172145]
56. Ripke S, O'Dushlaine C, Chambert K, Moran JL, Kahler AK, Akterin S et al. Genomewide association analysis identifies 13 new risk loci for schizophrenia. Nat Genet 2013; 45: 1150–1159. [PubMed: 23974872]
57. Hagger C, Buckley P, Kenny JT, Friedman L, Ubogy D, Meltzer HY. Improvement in cognitive functions and psychiatric symptoms in treatment-refractory schizophrenic patients receiving clozapine. Biol Psychiatry 1993; 34: 702–712. [PubMed: 8292674]
58. Nielsen RE, Levander S, Kjaersdam Telleus G, Jensen SO, Ostergaard Christensen T, Leucht S. Second-generation antipsychotic effect on cognition in patients with schizophrenia--a meta-

analysis of randomized clinical trials. Acta Psychiatr Scand 2015; 131: 185–196. [PubMed: 25597383]

59. Keefe RS, Silva SG, Perkins DO, Lieberman JA. The effects of atypical antipsychotic drugs on neurocognitive impairment in schizophrenia: a review and meta-analysis. Schizophr Bull 1999; 25: 201–222. [PubMed: 10416727]
60. Woodward ND, Purdon SE, Meltzer HY, Zald DH. A meta-analysis of neuropsychological change to clozapine, olanzapine, quetiapine, and risperidone in schizophrenia. Int J Neuropsychopharmacol 2005; 8: 457–472. [PubMed: 15784157]
61. Keefe RS, Bilder RM, Davis SM, Harvey PD, Palmer BW, Gold JM et al. Neurocognitive effects of antipsychotic medications in patients with chronic schizophrenia in the CATIE trial. Arch Gen Psychiatry 2007; 64: 633–647. [PubMed: 17548746]
62. Meltzer HY. Pharmacotherapy of cognition in schizophrenia. Curr Opin Behav Sci 2015; 4: 115–121.
63. Gottesman II, Gould TD. The endophenotype concept in psychiatry: etymology and strategic intentions. Am J Psychiatry 2003; 160: 636–645. [PubMed: 12668349]
64. Hasler G, Drevets WC, Gould TD, Gottesman II, Manji HK. Toward constructing an endophenotype strategy for bipolar disorders. Biol Psychiatry 2006; 60: 93–105. [PubMed: 16406007]
65. Faucher MA. Folic acid supplementation before and in early pregnancy may decrease risk for autism. J Midwifery Women Health 2013; 58: 471–472.
66. Jones P Schizophrenia after prenatal exposure to the Dutch hunger winter of 1944–1945. Arch Gen Psychiatry 1994; 51: 333–334. [PubMed: 8161294]
67. Hoek HW, Susser E, Buck KA, Lumey LH, Lin SP, Gorman JM. Schizoid personality disorder after prenatal exposure to famine. Am J Psychiatry 1996; 153: 1637–1639. [PubMed: 8942466]
68. St Clair D, Xu M, Wang P, Yu Y, Fang Y, Zhang F et al. Rates of adult schizophrenia following prenatal exposure to the Chinese famine of 1959–1961. JAMA 2005; 294: 557–562. [PubMed: 16077049]
69. Cao B, Wang DF, Xu MY, Liu YQ, Yan LL, Wang JY et al. Lower folate levels in schizophrenia: a meta-analysis. Psychiatry Res 2016; 245: 1–7. [PubMed: 27521746]
70. Wang D, Zhai JX, Liu DW. Serum folate levels in schizophrenia: a meta-analysis. Psychiatry Res 2016; 235: 83–89. [PubMed: 26652840]
71. Roffman JL, Lamberti JS, Achtyes E, Macklin EA, Galendez GC, Raeke LH et al. Randomized multicenter investigation of folate plus vitamin B12 supplementation in schizophrenia. JAMA Psychiatry 2013; 70: 481–489. [PubMed: 23467813]
72. Canever L, Alves CS, Mastella G, Damazio L, Polla JV, Citadin S et al. The evaluation of folic acid-deficient or folic acid-supplemented diet in the gestational phase of female rats and in their adult offspring subjected to an animal model of schizophrenia. Mol Neurobiol 2017; 1–20. [PubMed: 26708209]
73. van Os J Schizophrenia after prenatal famine. Arch Gen Psychiatry 1997; 54: 577–578. [PubMed: 9193199]
74. Pitkin RM. Folate and neural tube defects. Am J Clin Nutr 2007; 85: 285S–288SS. [PubMed: 17209211]
75. Bahous RH, Jadavji NM, Deng L, Cosín-Tomás M, Lu J, Malysheva O et al. High dietary folate in pregnant mice leads to pseudo-MTHFR deficiency and altered methyl metabolism, with embryonic growth delay and short-term memory impairment in offspring. Hum Mol Genet 2017; 26: 888–900. [PubMed: 28069796]
76. Kearney J Food consumption trends and drivers. Philos Trans R Soci Lond B Biol Sci 2010; 365: 2793–2807.

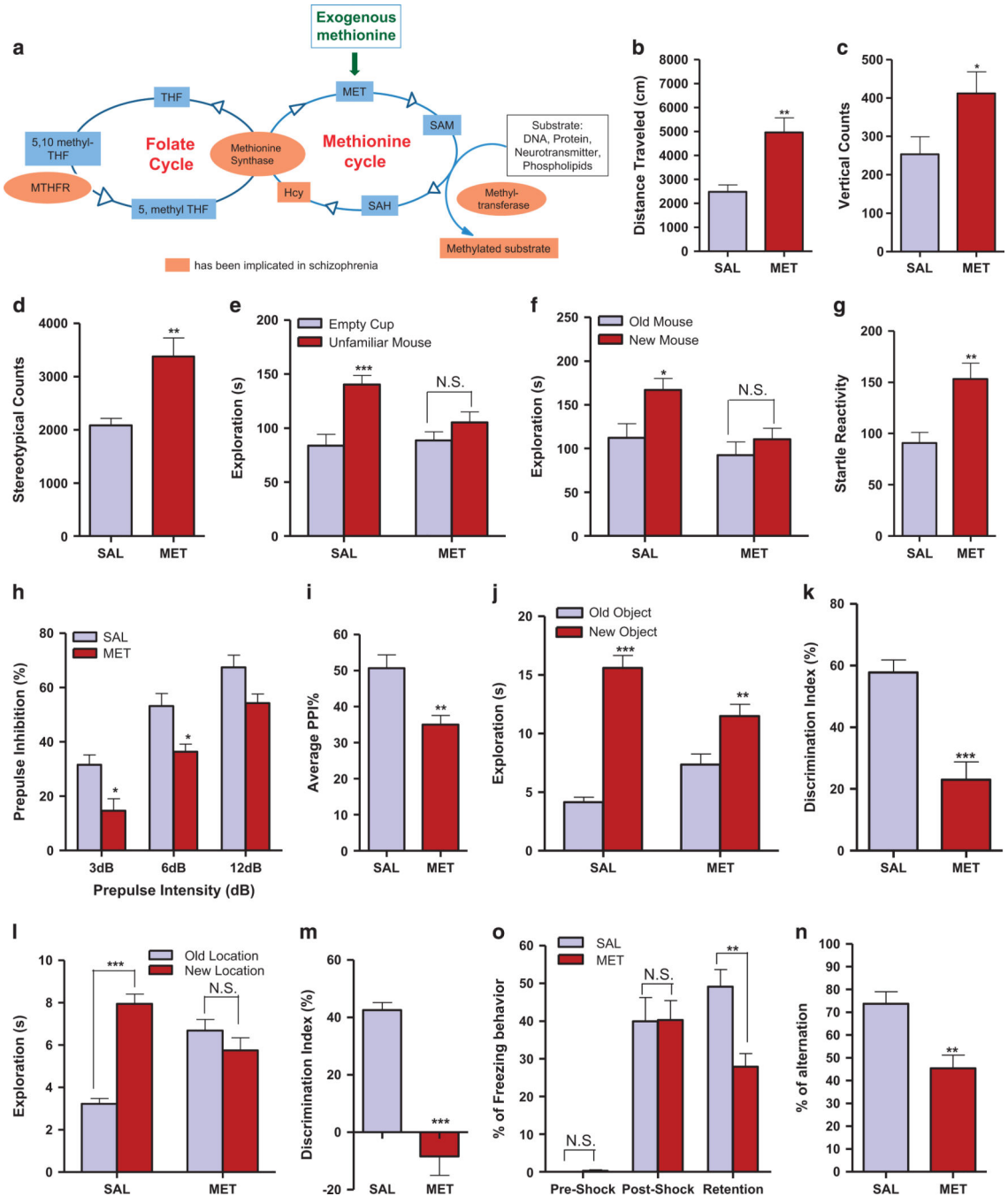

Figure 1.

MET mice display behavioral deficits and impairments that mimic schizophrenia symptoms. (**a**) Schematic overview of the methionine pathways and their interactions with the folate cycle. (**b**) Distance mice traveled in 60 min of the locomotion assay (n=11). Unpaired student test (t =3.622, P =0.0017): SAL versus MET, **P<0.01. Data are presented as means ± s.e.m. (**c**) Vertical counts in 60 min of the locomotion assay (n =11). Unpaired student test (t= 2.174, P =0.0419): SAL versus MET, *P<0.05. Data are presented as means ± s.e.m. (**d**) Stereotypic counts in 60 min of the locomotion assay (n=11). Unpaired student test (t

=3.497, P=0.0023): SAL versus MET, **P<0.01. Data are presented as means ± s.e.m. (**e**) Time mice spent interacting with empty cup and unfamiliar mouse in the social interaction assay (n =11 SAL, 10 MET). Two-way ANOVA revealed a significant object effect ($F_{1,38}$=15.44, P=0.0003) and drug × object interaction ($F_{1,38}$ =4.621, P=0.0380) followed by Bonferroni *post hoc* test: empty cup versus unfamiliar mouse, *** P<0.001, NS, not significant. Data are presented as means ± s.e.m. (**f**) Time mice spent interacting with old and new control mice in the social novelty assay (n=11 SAL, 10 MET). Two-way ANOVA revealed a significant drug effect ($F_{1,38}$ =6.914, P= 0.0123) and object effect ($F_{1,38}$ =6.293, P =0.0165) followed by Bonferroni *post hoc* test: old versus new control mouse, * P<0.05, NS, not significant. Data are presented as means ± s.e.m. (**g**) Startle reactivity to pulse stimulations in the PPI assay (n=13 SAL, 11 MET). Unpaired student test (t=3.459, P=0.0022): SAL versus MET, **P<0.01. Data are presented as means ± s.e.m. (**h**) Prepulse inhibition ratios against three prepulse stimulations in the PPI assay (n =13 SAL, 11 MET). Two-way ANOVA revealed a significant drug effect ($F_{1,66}$=22.25, Po0.0001) and prepulse effect ($F_{2,66}$=43.43, P<0.0001) followed by Bonferroni *post hoc* test: SAL versus MET, *P<0.05, NS, not significant. Data are presented as means ± s.e.m. (**i**) Average PPI ratio in the PPI assay (n =13 SAL and 11 MET). Unpaired student test (t= 3.396, P= 0.0026): SAL versus MET, **P<0.01. Data are presented as means ± s.e.m. (**j**) Time mice spent exploring both the new and old objects during test session in the NOR assay (n= 10 SAL, 12 MET). Two-way ANOVA revealed a significant object effect ($F_{1,40}$ = 73.97, P<0.0001) and drug × object interaction ($F_{1,40}$ = 16.31, P= 0.0002) followed by Bonferroni *post hoc* test: old object versus new object, ** P<0.01, *** P<0.001. Data are presented as means ± s.e.m. (**k**) Discrimination index in the NOR assay (n= 10 SAL, 12 MET). Unpaired student test (t=4.761, P=0.0001): SAL versus MET, ***P<0.001. Data are presented as means ± s.e.m. (**l**) Time mice spent exploring objects in both the new and old locations during test session in the LOR assay (n =12 SAL, 14 MET). Two-way ANOVA revealed a significant location effect ($F_{1,48}$=16.63, P=0.0002) and drug × object interaction ($F_{1,48}$=37.39, P<0.0001) followed by Bonferroni *post hoc* test: old location versus new location, *** P<0.001, NS, not significant. Data are presented as means±s.e.m. (**m**) Discrimination index in the LOR assay (n=10 SAL, 12 MET). Unpaired student test (t =7.580, P<0.0001): SAL versus MET, ***P<0.001. Data are presented as means ± s.e.m. (**n**) Percentage of freezing behavior in contextual fear conditioning assay (n=15 SAL, 12 MET). Two-way ANOVA revealed a significant drug effect ($F_{1,75}$=3.985, P=0.0496), stage effect ($F_{2,75}$=57.52, P<0.0001) and drug × stage interaction ($F_{2,75}$=4.311, P=0.0168) followed by Bonferroni *post hoc* test: SAL versus MET, ***P<0.001, NS, not significant. Data are presented as means ± s.e.m. (**o**) Percentage of the alternation choice mice made in the T maze spontaneous assay (n =12 SAL and 11 MET). Unpaired student test (t =3.667, P= 0.0014): SAL versus MET, ***P<0.001. Data are presented as means ±s.e.m.

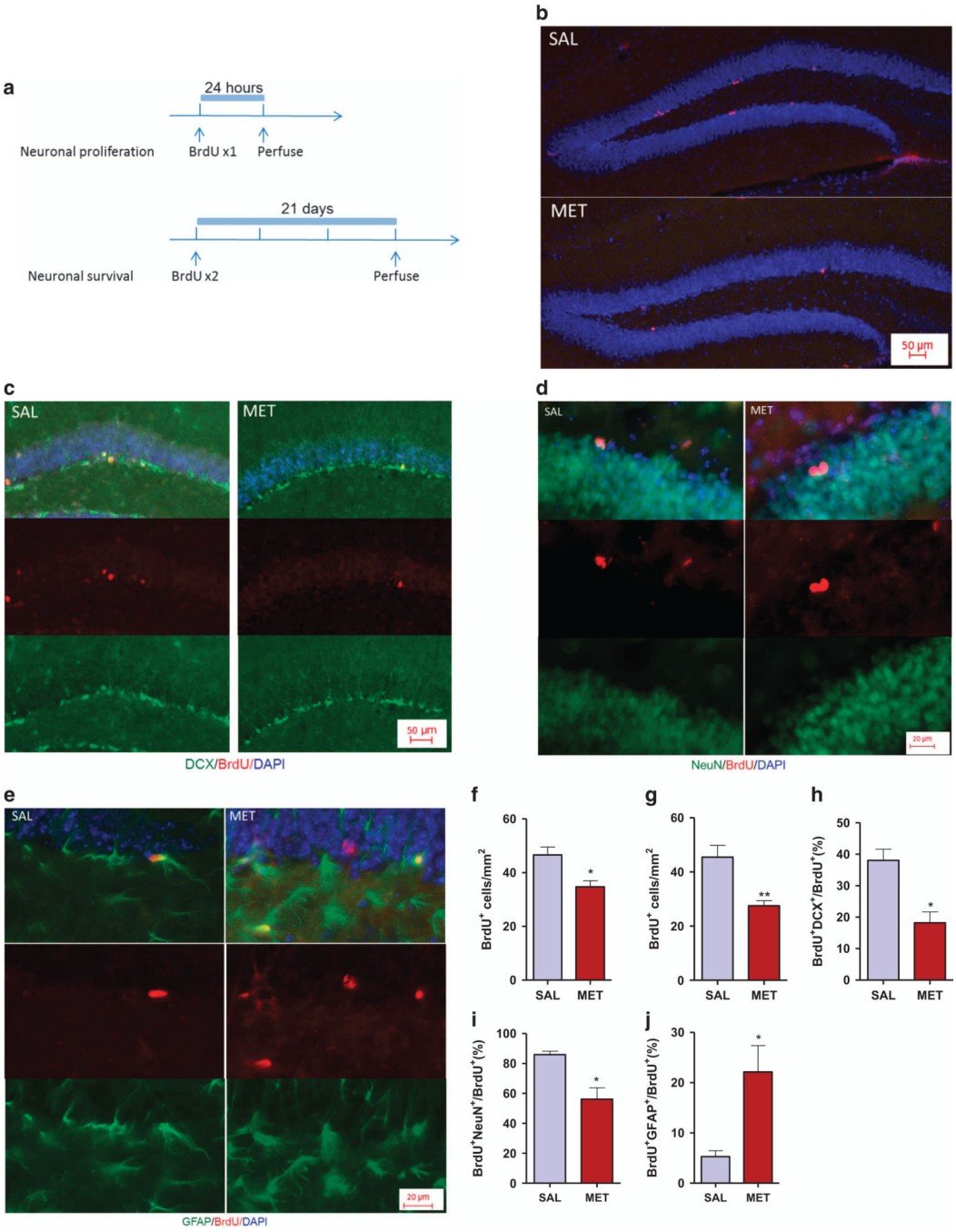

Figure 2.

MET mice display decreased proliferation and differentiation and increased gliogenesis. (**a**) Experimental design for BrdU administration. (**b**) Images of the hippocampus dentate gyrus showing BrdU (red) and DAPI (blue) staining at 24 h after injection of BrdU to SAL and MET pups. (**c**) Images of $BrdU^+/DCX^+$ cells showing BrdU and DCX immunoreactivity at 21 days after two BrdU injections. (**d**) Images of $BrdU^+/NeuN^+$ cells showing BrdU and NeuN immunoreactivity at 21 days after two BrdU injections. (**e**) Images of $BrdU^+/GFAP^+$ cells showing BrdU and GFAP immunoreactivity at 21 days after two BrdU injections. (**f**)

Quantification of BrdU-immunopositive cells at 24 h post-BrdU injection (n=3 mice per group). Unpaired student test (t=3.2, P=0.032): SAL versus MET, *P<0.05. Data are presented as means ± s.e.m. (g) Quantification of BrdU-immunopositive cells at 21 days post-BrdU injections (n=3 SAL, 4 MET). Unpaired student test (t=4.2, P=0.0084): SAL versus MET, **P<0.01. Data are presented as means ± s.e.m. (h) Number of new immature neurons ($BrdU^+/DCX^+$) in the dentate subgranular zone at 21 days after two BrdU injections (n=3 SAL, 4 MET). Unpaired student test (t=3.92, P=0.011): SAL versus MET, *P<0.05. Data are presented as means ± s.e.m. (i) Number of new immature neurons ($BrdU^+/NeuN^+$) in the dentate subgranular zone at 21 days after two BrdU injections (n=3 SAL, 4 MET). Unpaired student test (t=3.38, P=0.012): SAL versus MET, *P<0.05. Data are presented as means ± s.e.m. (j) Number of new astrocytes ($BrdU^+/GFAP^+$) in the dentate subgranular zone at 21 days after two BrdU injections (n=3 mice per group). Unpaired student test (t=3.14, P=0.0348): SAL versus MET, *Po0.05. Data are presented as means ± s.e.m.

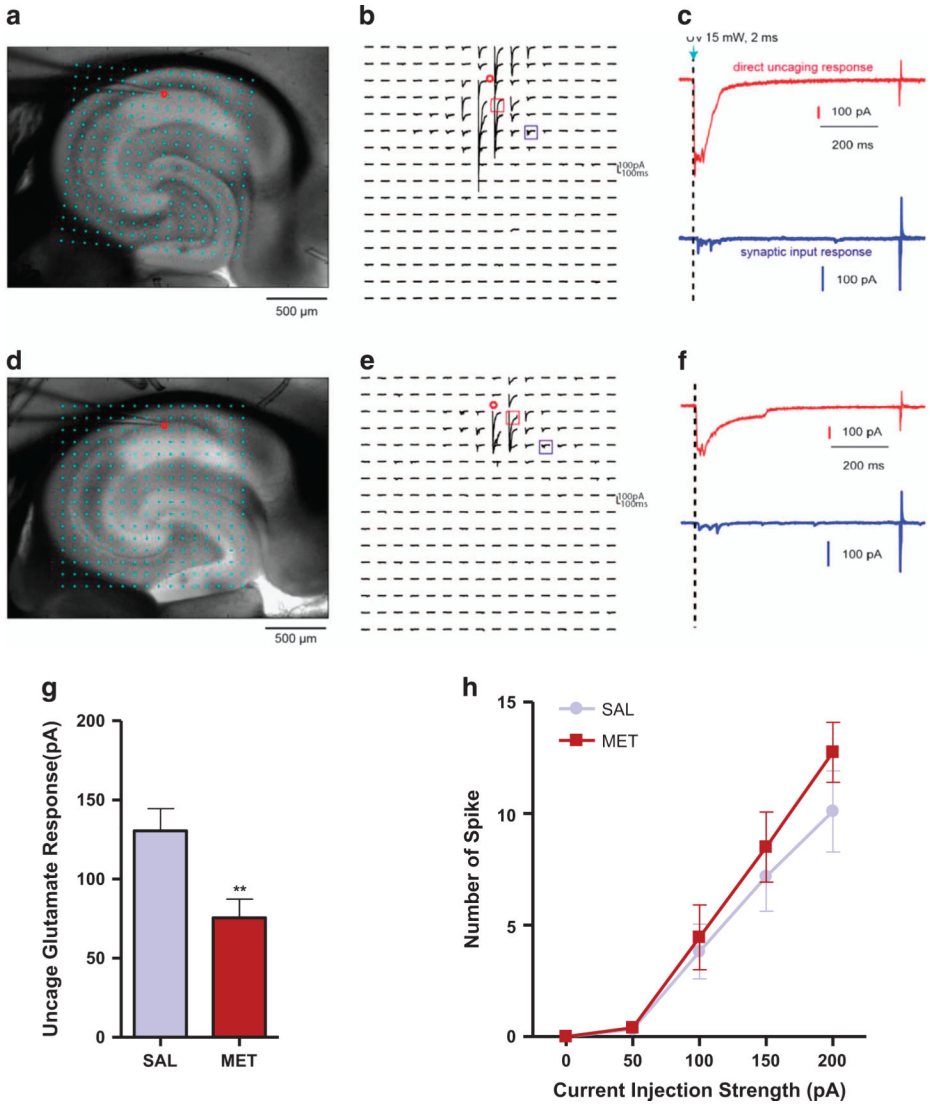

Figure 3.

MET mice exhibit reduced local excitatory synaptic connections of the CA1 excitatory. (**a**) Exemplar hippocampal slice image from SAL group with the superimposed photostimulation sites (16 × 16 cyan dots). The red circle indicates the somatic location of the recorded pyramidal neuron. Stimulation sites are spaced at 90 μm × 90 μm. This distance has been empirically determined to capture the smallest predicted distance in which photostimulation differentially activates adjacent neurons and to avoid overlap of the laser-illuminated area. During the experiment, the slice is bathed in the solution containing MNI-caged glutamate, which only turns active through focal UV photolysis to activate a small number of neurons (that is, glutamate uncaging). (**b**) Example of photostimulation-evoked response traces from SAL group in most sites shown at (**a**), with the recorded cell held at − 70 mV in voltage clamp mode to detect inward excitatory postsynaptic currents. The small red circle indicates the recorded cell body location. Only the 200 ms of the response traces after laser photostimulation (15 mW, 2 ms) are shown. Different forms of photostimulation-evoked responses are illustrated by the traces of red and blue cube, expanded and separately

shown as the red and blue traces. (**c**) The red trace is an example of the direct response to glutamate uncaging on the cell body (excluded for further analysis) from SAL group, which can be distinguished by its large amplitude and short latency. The blue trace is a typical example of synaptic input responses. (**d**) Example of a hippocampal slice image from methionine group with the superimposed photostimulation sites. The red circle indicates the somatic location of the recorded pyramidal neuron. (**e**) Example of photostimulationevoked response traces from methionine group in most sites shown at (**d**). The small red circle indicates the recorded cell body location. Different forms of photostimulation-evoked responses are illustrated by the traces of red and blue cube, expanded and separately shown as the red and blue traces in (**f**). (**f**) The red trace is an example of the direct response to glutamate uncaging on the cell body (excluded for further analysis) from methionine group. The blue trace is a typical example of synaptic input responses. (**g**) Quantitative analysis of the average uncaging responses by measuring evoked postsynaptic currents upon photostimulation on CA 1 pyramidal neurons of SAL and MET group (n=11–13 slices, n=3 SAL, 4 MET). Unpaired student test (t=2.937, P= 0.0076): SAL versus MET, **P<0.01. Data are presented as means ± s.e.m. (h) Intrinsic membrane excitability measured by the overall relationship of spiking number versus intrasomatic current injection strength on CA 1 pyramidal neurons of SAL and MET group (n=11–12 slices, n=3 SAL, 4 MET). Two-way ANOVA revealed no significant drug effect ($F_{1,105}$=1.602, P=0.2085). Data are presented as means ± s.e.m.

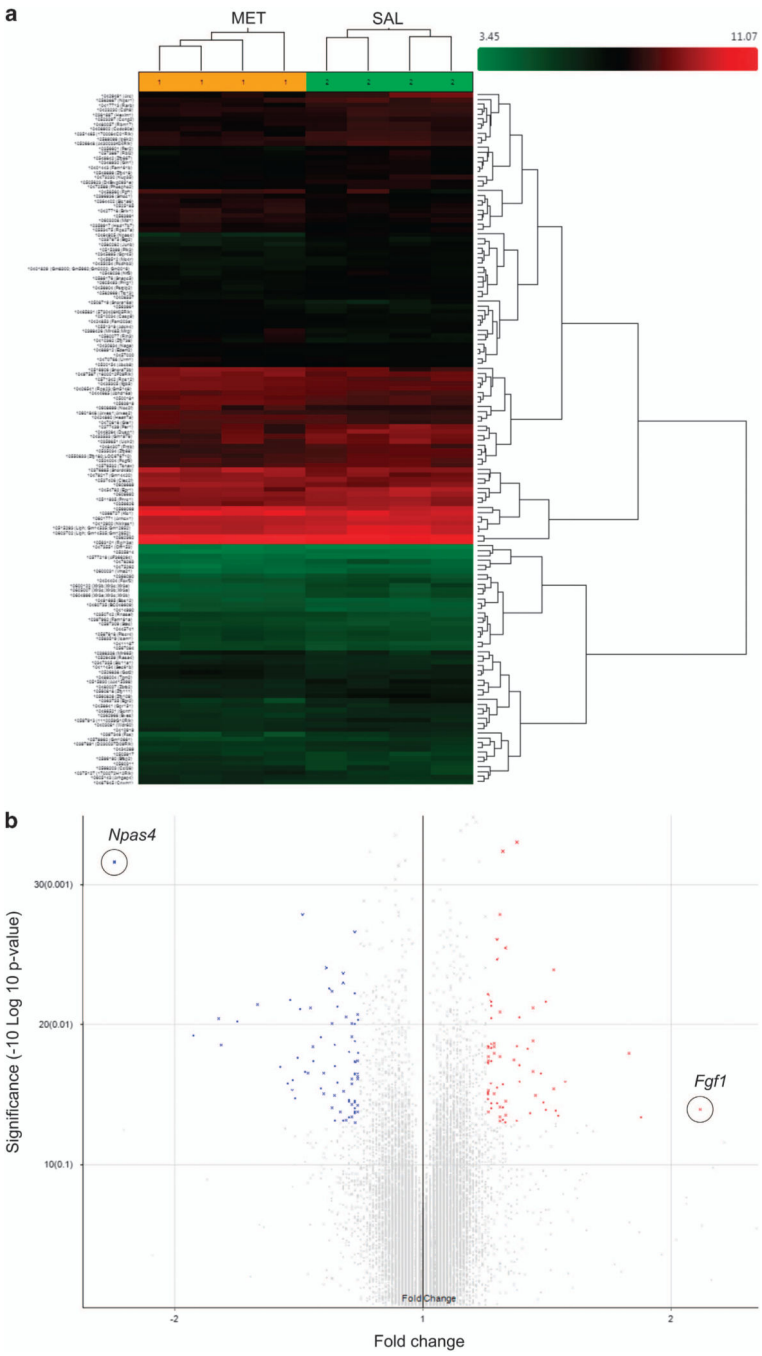

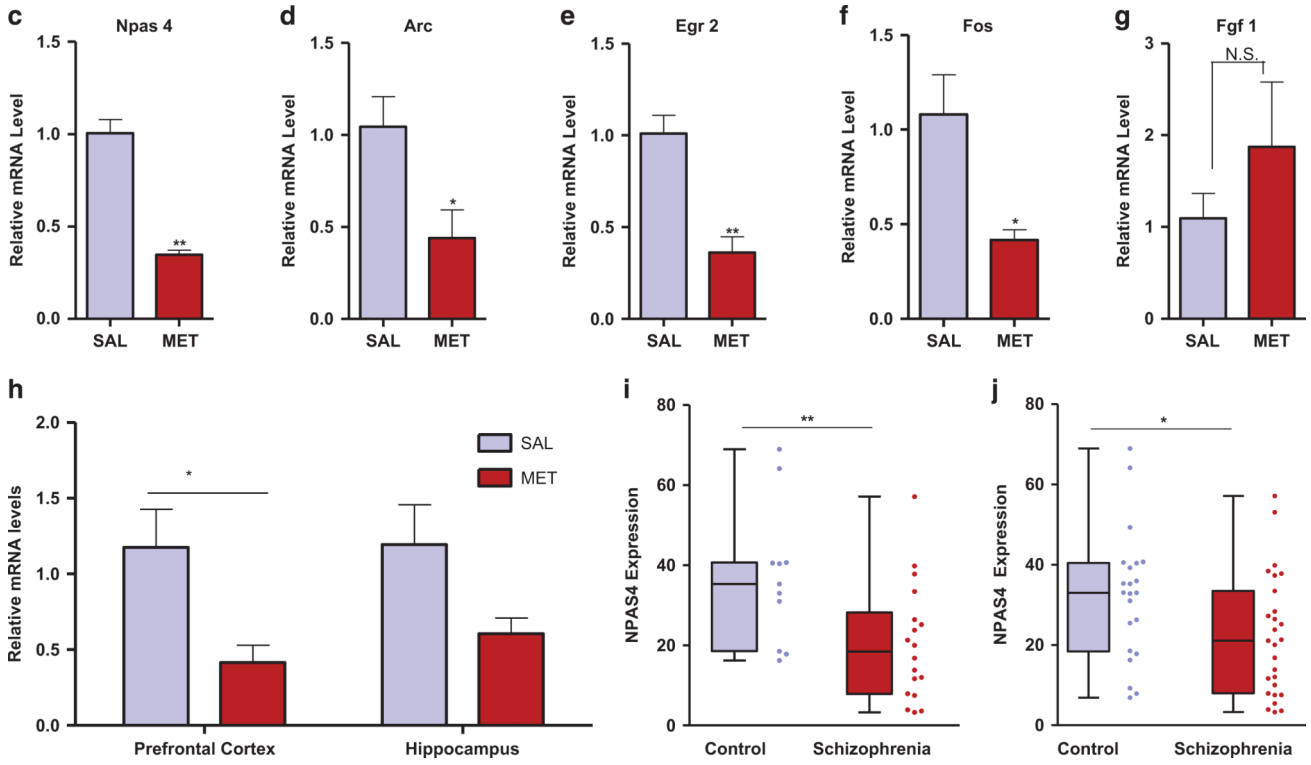

Figure 4.

Downregulation of neuronal immediate early genes in MET mice and human schizophrenics. (**a**) Hierarchical clustering analysis of differentially expressed genes (>1.2-fold change, $P<0.05$) in brains from MET versus SAL mice. (**b**) Volcano plot showing differentially expressed genes in brains from MET versus SAL mice. Npas4 (circled) exhibited the largest expression change among the downregulated genes (blue symbols); *Fgf1* (circled) exhibited the largest expression change among the upregulated genes (red symbols). (**c-g**) Real-time qPCR validation of microarray. Relative global mRNA levels of NPAS4 (**c**), Arc (**d**), Egr2 (**e**), Fos (**f**) and Fgf1 (**g**) genes in the mice brain assessed by quantitative real-time PCR (n= 3–4). Unpaired student test (Npas4: t =8.444, P =0.0011; Arc: t=2.684, P=0.0363; Egr2: t =4.977, P=0.0042; Fos: t=3.05. P=0.037, Fgf1: t=1.026, P= 0.3444): SAL versus MET, *$P<0.05$, **$P<.01$, NS, not significant. Data are presented as means ± s.e.m. (**h**) qT-PCR analysis of NPAS4 mRNA expression in the prefrontal cortex (n=7), hippocampus (n= 7 SAL, 6 MET). Two-way ANOVA revealed a significant drug effect ($F_{1,23}$ = 10.9, P=0.0123) but no significant subregional effect ($F_{1,23}$ = 0.25, P40.05) followed by Bonferroni *post hoc* test: SAL versus MET in the prefrontal cortex, (t= 2.686, $P<0.05$), SAL versus MET in the hippocampus, (t= 1.99, P40.05). *$P<0.05$, Data are presented as means ± s.e.m. Data are presented as means ± s.e.m. (**i, j**) Npas4 mRNA expression in the anterior prefrontal cortex (Brodmann Area 10) of post-mortem patients with schizophrenia and control subjects. Box and whisker plot of gene expression of (**i**) male (n =18 male patients and 11 male matched controls) and (**j**) total (n=27 schizophrenia patients and 22 matched controls), Empirical Bayes moderated t-test (male: P= 0.007, total: P= 0.0189): control versus schizophrenia, *$P<0.05$, **$P<0.01$.

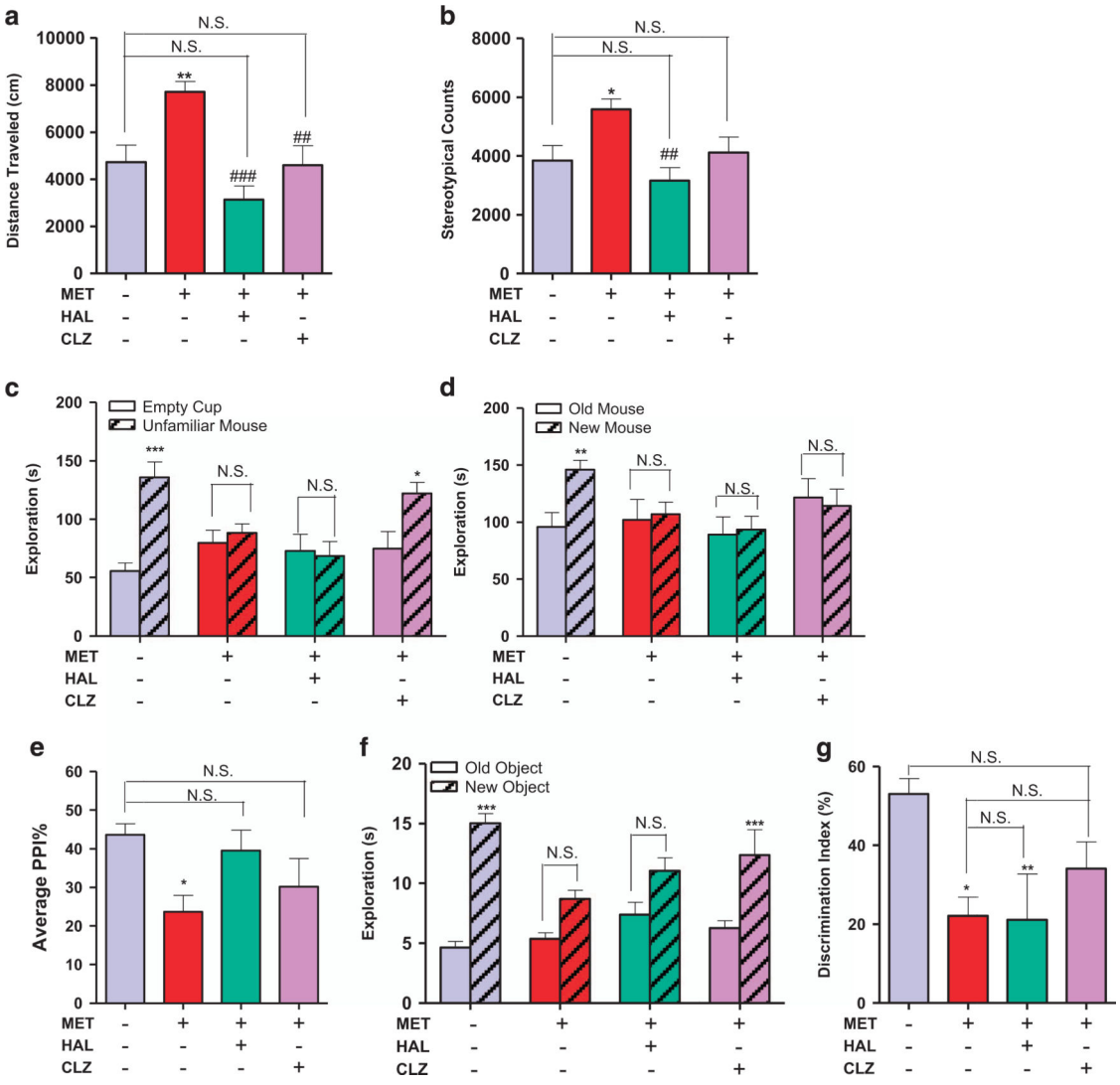

Figure 5.

Antipsychotics differentially alleviate the behavioral deficits in MET mice. (a) Effect of haloperidol (0.1 mg/kg, i.p.) and clozapine (1.0 mg/kg, i.p.) on locomotor hyperactivity in the prenatal methionine overload male offspring (n=8 SAL, 9 MET, 9 CLZ, 8 sHAL). One-way anovas revealed a significant drug effect ($F_{3,30}$ = 9.417, P=0.0002) followed by Dunnett's *post hoc* test: SAL versus other three groups, ** P<0.01, NS, not significant; MET versus other three groups: $^{\#\#}P$<0.01, $^{\#\#\#}P$<0.001. Data are presented as means ± s.e.m. (**b**) Effect of haloperidol (0.1 mg/kg, i.p.) and clozapine (1.0 mg/kg, i.p.) on enhanced stereotypy in the prenatal methionine overload male offspring (n=8 SAL, 9 MET, 9 CLZ, 8 HAL). One-way ANOVAs revealed a significant drug effect ($F_{3,30}$=5.240, P=0.0050) followed by Dunnett's *post hoc* test: SAL versus other three groups, * P<0.05, NS, not significant; MET versus other three groups: $^{\#\#}P$<0.01 Data are presented as means ± s.e.m. (**c**) Effect of haloperidol (0.1 mg/kg, i.p.) and clozapine (1.0 mg/kg, i.p.) on social withdraw in the prenatal methionine overload male offspring (n=9). Two-way ANOVA revealed a significant object effect ($F_{1,64}$=16.46, P=0.0001) and drug × object interaction ($F_{1,38}$=5.560,

P=0.0019) followed by Bonferroni *post hoc* test: empty cup versus unfamiliar mouse, *P<0.05, ***P<0.001, NS, not significant. Data are presented as means ± s.e.m. (**d**) Effect of haloperidol (0.1 mg/kg, i.p.) and clozapine (1.0 mg/kg, i.p.) on social recognition deficit in the prenatal methionine overload male offspring (n=9). Two-way ANOVA revealed no significant object effect ($F_{1,64}$=1.785, P=0.1863) followed by Bonferroni *post hoc* test: old versus new control mouse, **P<0.01, NS, not significant. Data are presented as means ± s.e.m. (e) Effect of haloperidol (0.25 mg/kg, i.p.) and clozapine (2.5 mg/kg, i.p.) on PPI deficit in the prenatal methionine overload male offspring (n=18 SAL, 19 MET, 16 ClZ, 16 HAL). One-way ANOVAs revealed a significant drug effect ($F_{3,65}$=3.331, P=0.0248) followed by Dunnett's *post hoc* test: SAL versus other three groups, *P<0.05, NS, not significant; MET versus other three groups, NS, not significant. Data are presented as means ± s.e.m. (**f**) Effect of haloperidol (0.1 mg/kg, i.p.) and clozapine (1.0 mg/kg, i.p.) on object recognition deficit in the prenatal methionine overload male offspring (n=9). Two-way ANOVA revealed a significant drug effect ($F_{3,64}$=2.791, P=0.0475), object effect ($F_{1,64}$=62.28, P<0.0001) and drug × object interaction ($F_{3,64}$=4.775, P=0.0046) followed by Bonferroni *post hoc* test: old object versus new object, ***P<0.001, NS, not significant. Data are presented as means ± s.e.m. (**g**) Effect of haloperidol (0.1 mg/kg, i.p.) and clozapine (1.0 mg/kg, i.p.) on the discrimination index of the NOR assay in the prenatal methionine overload male offspring (n=9). One-way ANOVAs revealed a significant drug effect ($F_{3,28}$=4.481, P=0.109) followed by Dunnett's *post hoc* test: SAL versus other three groups, *P<0.05, **P<0.01, NS, not significant; MET versus other three groups, NS, not significant. Data are presented as means ± s.e.m.